Progress In Electromagnetics Research C, Vol. 41, 201–215, 2013

A FUNCTIONAL ANTENNA TUNER FOR SLOT PATCH ANTENNA

Chia-Ching Chu[1], Lih-Shan Chen[1], Hsien-Chiao Teng[2], and Shen Cherng[3, *]

[1]Department of Electronic Engineering, I-Shou University, No. 1, Sec. 1, Xuecheng Rd., Dashu Dist., Kaohsiung City 840, Taiwan

[2]Department of Electrical Engineering, ROC Military Academy, No. 1, Weiwu Rd., Fengshan Dist., Kaohsiung City 830, Taiwan

[3]Computer Science and Information Engineering, Chengshiu University, No. 840, Chengqing Rd., Niaosong Dist., Kaohsiung City 833, Taiwan

Abstract—In this paper, without using external power and active components, a design of pin coupled functional antenna tuner is presented. The tuner consists of two parts, a coupling pin and a tuning circuit. It is used to tune the bandwidth and antenna gain of the proposed slot patch antenna. The prototype, including a slot patch antenna and the tuner, was constructed and excited through a T-shape microstrip feed circuit resonated at 2.6 GHz. The impedance bandwidth BW (−10 dB return loss) of the slot patch antenna without coupling to the tuner was 3% referred to the operation frequency at 2.6 GHz. When the tuner was matched with the impedance 75 Ω through the coupling pin to the proposed antenna, the BW of the antenna was increased to 11% operated at 2.6 GHz. However, if the tuner was matched with the impedance 25 Ω to the proposed slot patch antenna, the impedance bandwidth of the antenna was increased 21% at operation frequency. Relatively uniform antenna gain was obtained when the matching impedance was decreased from 75 Ω to 20 Ω. In the meantime, the lower matching impedance corresponds to more reducing cross-polarization of the proposed slot patch antenna can be observed in the measured field patterns.

Received 3 June 2013, Accepted 6 July 2013, Scheduled 9 July 2013

* Corresponding author: Shen Cherng (cherng@msu.edu).

1. INTRODUCTION

Microstrip antenna has advantages of low profile, low cost and easy integration to the microstrip circuits [1, 2] but disadvantages of low bandwidth [3]. Since microstrip antenna with wide bandwidth is very important for Wireless-LNA, Bluetooth and Video-interface [4], techniques of modifying bandwidth have been developed a lot. Structurally, it includes integrating several microstrip resonance structures into one antenna [5, 6], adding more structural layers to antenna [7], changing dielectric constant of substrate [8, 9], modifying probe feed structure [10–14] and printing functional slot to the radiator as well as the ground [15–18], etc. Lately, by using of stepped [19, 20] and slotted ground [21–23] for size reduction, parasitic elements for shorting the patch [24–26] to modify the bandwidth of microstrip antenna has been reported. In this study, the functional tuner which is used to improve the power transfer by matching the varied impedances, was designed and analyzed to regulate the bandwidth and gain of the antenna for the applications to WiMAX Ap system in the band of 2.5 GHz (2.5–2.69 GHz) [27, 28].

2. DESIGN CONFIGURATION

The schematic of the slot patch antenna studied is shown in Figure 1(a). The constructed prototype was implemented on a FR4 substrate ($\varepsilon_r = 4.4$) with the overall size of $69.5 \times 51 \times 1.6\,\text{mm}^3$. A

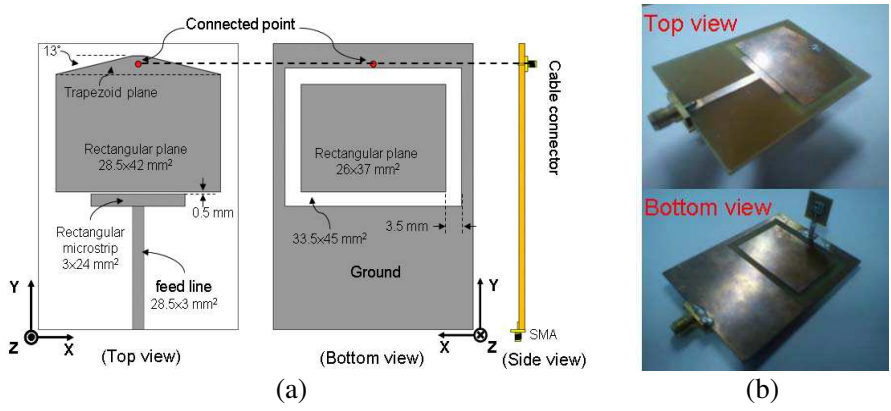

Figure 1. (a) Schematic drawing of slot patch antenna with a removable parasitic tuner module. (b) Constructed prototype of the slot patch antenna with the tuner.

slot line ($33.5 \times 45\,\text{mm}^2$) and a microstrip ($26 \times 37\,\text{mm}^2$) being coupled through the gap (3.5 mm) were printed on the ground. A T-shape probe-fed circuit includes two microstrip components with the sizes of $28.5 \times 3\,\text{mm}^2$ and $3 \times 24\,\text{mm}^2$. The operation frequency was designed at 2.6 GHz with the impedance bandwidth (−10 dB return loss) for the studied antenna The tuner was pin-coupled to the rectangular microstrip patch ($28.5 \times 42\,\text{mm}^2$) by using of a M17/113-RG316 cable line [29]. The length 1.5 cm of the cable line was used. The constructed prototype of the antenna with tuner is show in Figure 1(b).

Rectangular microstrip $24 \times 3\,\text{mm}^2$ is connected to the feed line (signal transmission line) of microstrip $28.5 \times 3\,\text{mm}^2$ and gap (0.5 mm) coupled to the rectangular plane $28.5 \times 42\,\text{mm}^2$, the probe-fed input matching impedance is 50 Ω to the slot patch antenna. The optimized return loss was obtained by adjusting of the length of transmission line and the width of rectangular microstrip. Figures 2(a) and 2(b) shows the measured return loss. As in figures, when the length of the rectangular microstrip was increased from 24 mm to 42 mm, the return loss at 2.6 GHz was changed from −7 dB to −16 dB. In contrast, when the width of the rectangular microstrip was reduced from 3 mm to 1 mm, the return loss was changed correspondingly as well. Therefore, the size of the rectangular microstrip for the slot patch antenna is optimized to be $24 \times 3\,\text{mm}^2$.

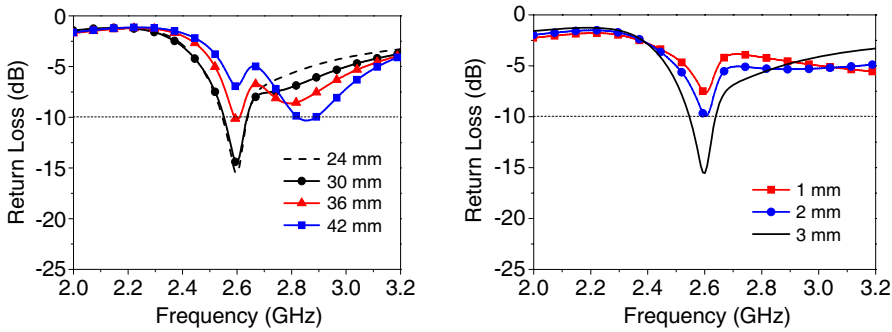

Figure 2. Measured results of RL with different values of (a) the length and (b) the width of rectangular microstrip.

In Figures 3(a) and 3(b), simulation results (by Ansoft HFSS10) show the surface currents on the patch (rectangular plan). The pro-feed T-shape microstrip transmitted current distribution could be adjusted by the angle θ at the connection point which is pin coupled to the tuner for matching impedance.

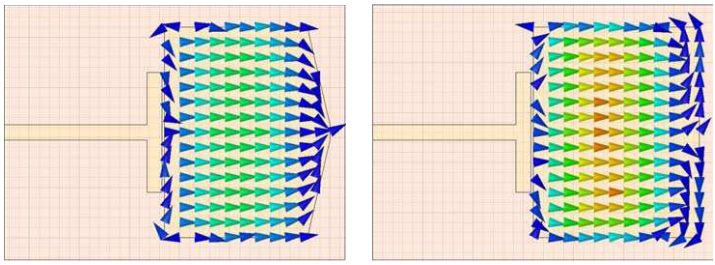

(a) (b)

Figure 3. Comparisons of surface currents (Ansoft HFSS10 simulation results) on the microstrip $l_3 \times w_3$ with the shape of (a) trapeziform and (b) rectangular.

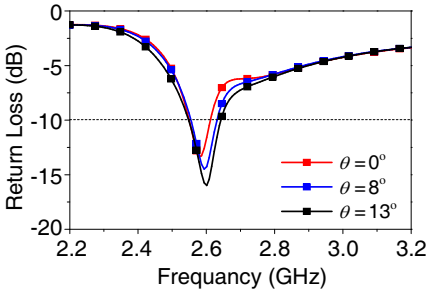

Figure 4. Measured results of RL with different values of the angle θ.

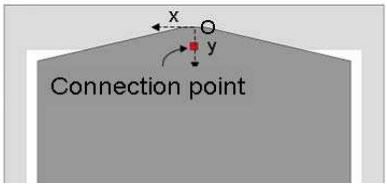

Figure 5. Geometry of the connection point and coordinate origin O.

Figure 4 shows modification of the return loss with the values of angle θ. As in Figure 4, the angle θ is determined to be 13° based upon the best value of the measured return loss.

In Figure 5, schematic drawing of the connection point design for a square pin (location of pin-coupling) with cross section of $1 \times 1\,\text{mm}^2$ is demonstrated. For the coordinate origin O was defined to be (0, 0) shown in the Figure 5, the output peak voltage at different locations with different coordinates of $y = 1\,\text{mm}$, 3 mm and 5 mm to the origin O responded to the input power of 30 dBm (calculated by Ansoft HFSS10) was 4.56 V, 3.16 V and 2.34 V respectively. On the other hand, if the coordinates of $x = 0\,\text{mm}$, 2 mm and 4 mm, the output peak voltage to the tuner is 3.16 V, 3.17 V and 2.86 V respectively. In this study, the coordinate of the coupling point is located at $x = 0\,\text{mm}$ and $y = 3\,\text{mm}$ to the coordinate origin point O, the output peak voltage to

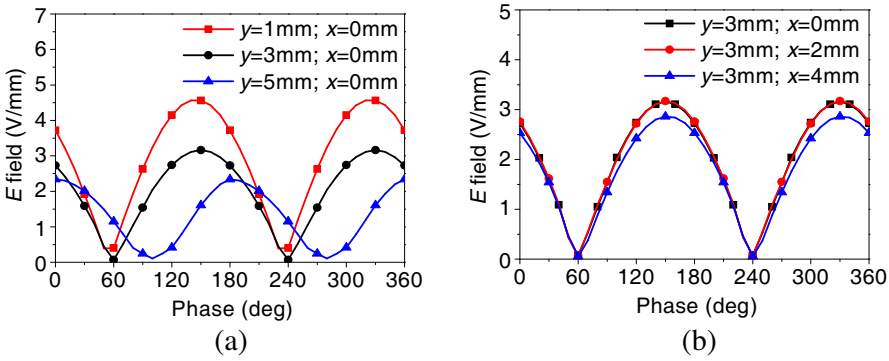

Figure 6. Probe-fed of 30 dBm power at the connection point, the voltage phase distribution is shown (a) with y-coordinate at $x = 0$ (b) with x-coordinate at $y = 3$ mm to the coordinate origin point O. (calculate by Ansoft HFSS10).

the tuner was thus 3.16 Volt which is shown in Figures 6(a) and 6(b).

In Figure 7(a), four different matching impedance designs of the tuner are presented. In the circuit of matching impedance at 25 Ω and 30 Ω, C_1 was designed to 1.5 pF that includes two 1 pF series connected capacitors and a parallel connected 1 pF capacitor. In the design of matching impedance at 75 Ω, C_1 is consists of six pieces of 1 pF capacitors series and parallel connected to catch 0.75 pF. However, in the circuit of matching impedance at 75 Ω, L_1 includes two pieces of inductance of 1.6 nH being parallel connected to catch 0.8 nH. At matching impedance of 25 Ω, the L_2 circuit includes 2 pieces conductance of 1.6 nH parallel connected to catch 0.8 nH. As shown in Figure 9(b), the functional tuner was constructed by using of the circuits printed on FR4 plate with the thickness of 0.4 mm being welded with inductance of SMD 0603 as well as capacitors and resistors. The constructed prototype of the tuner is demonstrated in Figure 7(c).

Basically, the tuner consists of four passive components L_1, C_1, L_2 and R_1 operated at 2.6 GHz with matching impedance 25 Ω, 30 Ω, 50 Ω and 75 Ω to regulate the power transfer from the pro-fed circuit. Components of the tuner circuits used for impedance matching are listed in Table 1.

The Smith charts of matching impedance for the tuner are shown in Figure 8. It demonstrates three steps to match the impedance. First, determine the characteristic impedance Z_0 when the source current goes through cable to L_1. Then, Z_0 is modified to Z_1 along with the path marked as '1' with colour red in Figure 8. Secondly, when the

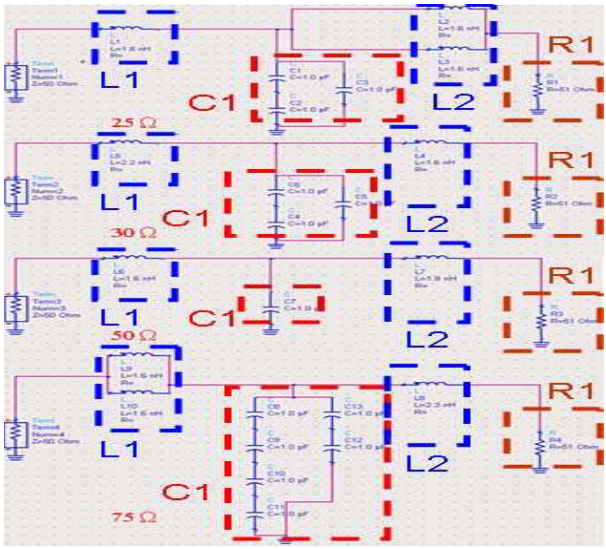

(a)

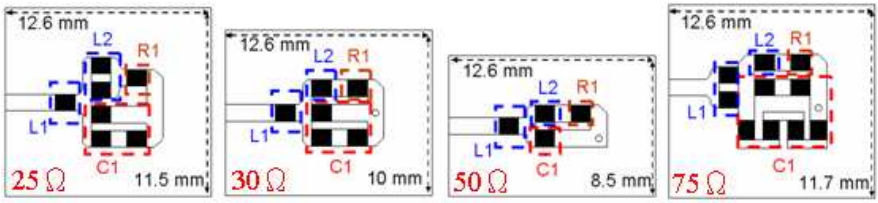

(b)

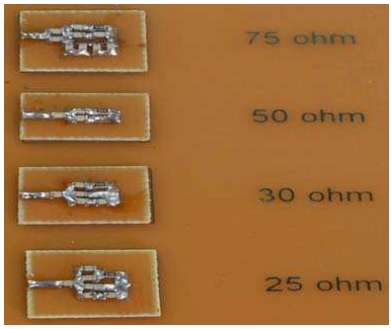

(c)

Figure 7. (a) Defined the tuner components in equivalent circuits. (b) Schematic drawing of the design of the circuits. (c) Constructed prototype of the tuner operated at 2.6 GHz.

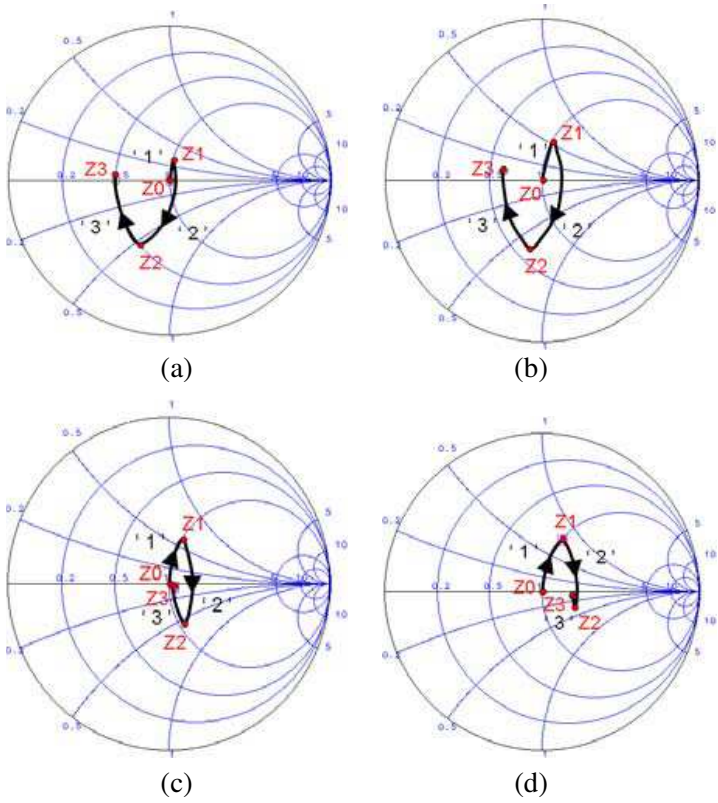

Figure 8. Smith charts of matching impedance at (a) 25 Ω, (b) 30 Ω, (c) 50 Ω, (d) 75 Ω for the microstrip slot patch antenna parallel connected to the tuner.

Table 1. Reactance of the components of the tuner at matching impedance in Figure 8.

Impedances	Re.	Im.	Re.	Im.	Re.	Im.	Re.	Im.
Z_0	51	0	51	0	51	0	51	0
Z_1	51.0	13.1	51.0	26.1	51.0	29.4	51.0	37.6
Z_2	25.2	−27.1	30.2	−32.1	52.9	−28.2	74.8	−17.0
Z_3	**25.2**	2.3	**30.2**	3.8	**52.9**	−2.1	**74.8**	−3.9

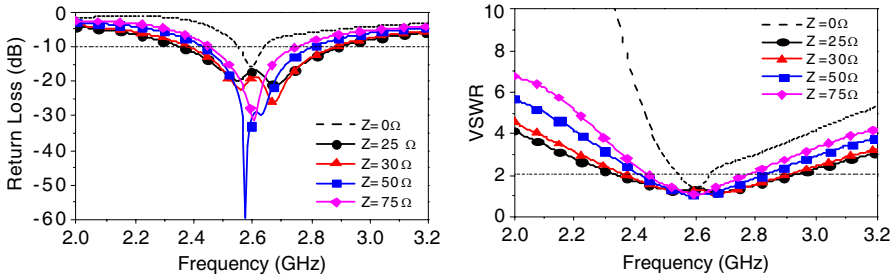

Figure 9. Measured results of (a) VSWR, (b) return Loss for the constructed prototype of the proposed antenna with different impedance matching to the tuner.

current goes through L_1 to the microstrip C_1, Z_1 is modified to Z_2 along with the path marked as '2' with colour blue. Finally, when the current goes through C_1 to the microstrip L_2, Z_2 is modified to Z_3 along with the path marked as '3' with colour black. Through the pin-coupling, the microstrip tuner can access the power from the probe-fed circuit to the slot patch antenna and then be activated to operate at 2.6 GHz with matching impedance 25 Ω, 30 Ω, 50 Ω and 75 Ω correspondingly.

Details of the impedance characteristics of each component on the tuner circuit are calculated by using of software ADS2008 and are given in Table 2.

Table 2. Components of the circuit for the tuner used for matching impedance.

Impedance matched [Ω]	L_1 [nH]	C_1 [pF]	L_2 [nH]	R_1 [Ω]
25	1.8	1.5	0.8	51
30	2.2	1.5	1.6	51
50	1.6	1	1.8	51
75	0.8	0.75	2.3	51

3. MEASUREMENTS AND SIMULATIONS

The measured return loss and voltage standing wave ratio (VSWR) of the antenna studied are shown in Figures 9(a) and 9(b). The bandwidth BW of the slot patch antenna was demonstrated 3% without coupling of the tuner. The BW of the antenna was improved

to 11% when the tuner was pin-coupled to provide 75 Ω impedance matching to the slot patch microstrip antenna. Comparatively, when the tuner was pin-coupled to the slot patch with matching impedance 50 Ω, 30 Ω and 25 Ω, the BW of the antenna would be increased to 14%, 18% and 21% correspondingly. The measured BW of constructed prototype is listed in Table 3.

Table 3. The measured BW of the slot patch microstrip antenna with the tuner.

Matching Impedance [Ω]	Return Loss [dB]	BW [%]
0	16	3
25	17	21
30	19	18
50	30.36	14
75	30.42	11

The equivalent circuit of slot patch microstrip antenna was calculated by using of Smith Chart Tool in the software ADS. In this study, two parts are comprised to analyze the equivalent circuit. Part 1 is the equivalent circuit of slot patch microstrip antenna without the tuner. Part 2 is the equivalent circuit load Z_L for the antenna which is the impedance of the tuner. In Figure 10, the equivalent circuits of the slot patch microstrip antenna with the tuner are demonstrated in part 3. If the matching impedance $Z = 75\,\Omega$, the equivalent circuit of

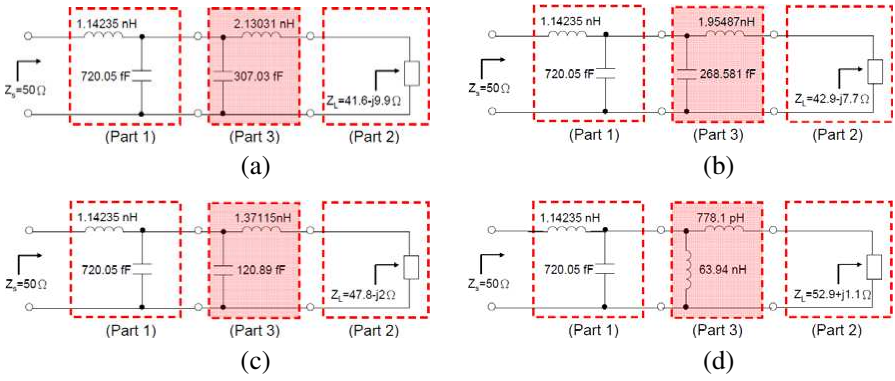

Figure 10. The calculated equivalent circuits of (a) 25 Ω, (b) 30 Ω, (c) 50 Ω, (d) 75 Ω matching impedance from the slot patch antenna to the functional tuner.

the slot patch microstrip antenna with the tuner is proposed with the parallel connecting of two inductors. In comparison, when $Z = 30\,\Omega$ and $Z = 50\,\Omega$, the equivalent circuit consists of a series connected inductor and a parallel connected capacitor.

The radiation pattern defines the variation of the power radiated by an antenna. It is described as a function of the direction from the antenna. In Figure 11, the measured field patterns of the proposed antenna are demonstrated. The tuner circuit with different values of matching impedance to the slot patch antenna does not change the radiation patterns specifically. The structure of the antenna is the major factor to dominate the radiation patterns. The studied slot patch antenna was originally designed with the maximum radiation patterns along the $+Z$ axis [30–32], however, the rectangular slot line reversely creates the maximum radiation pattern occurring along the $-Z$ axis [33, 34]. Generally, it is defined the radiation E plane is the YZ plan. H plane is the XZ plan. Therefore, co-polarization planar

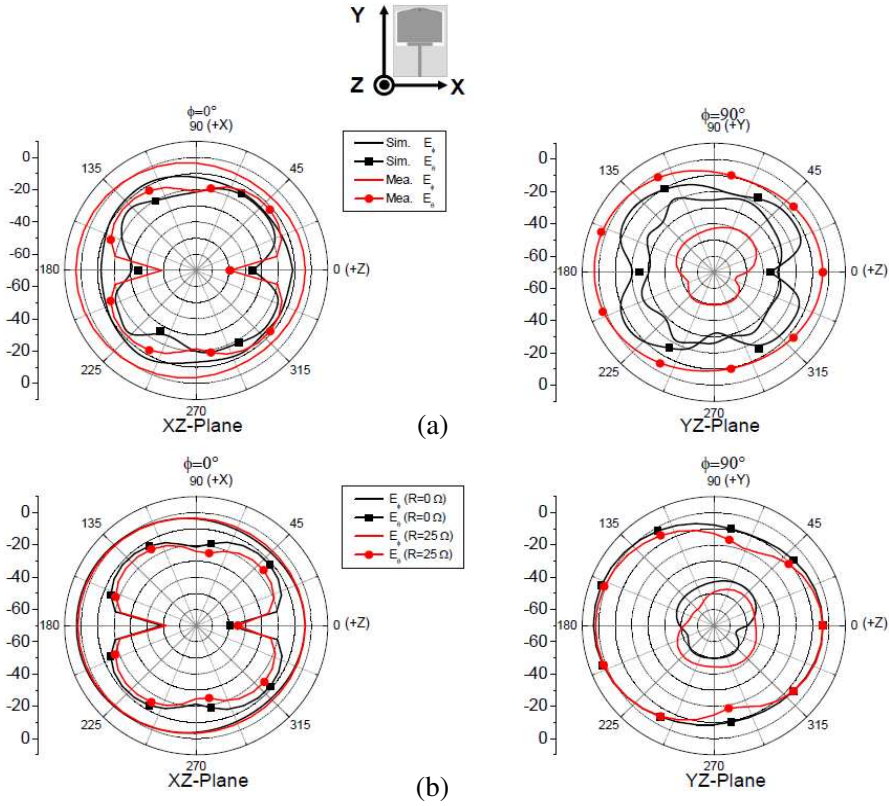

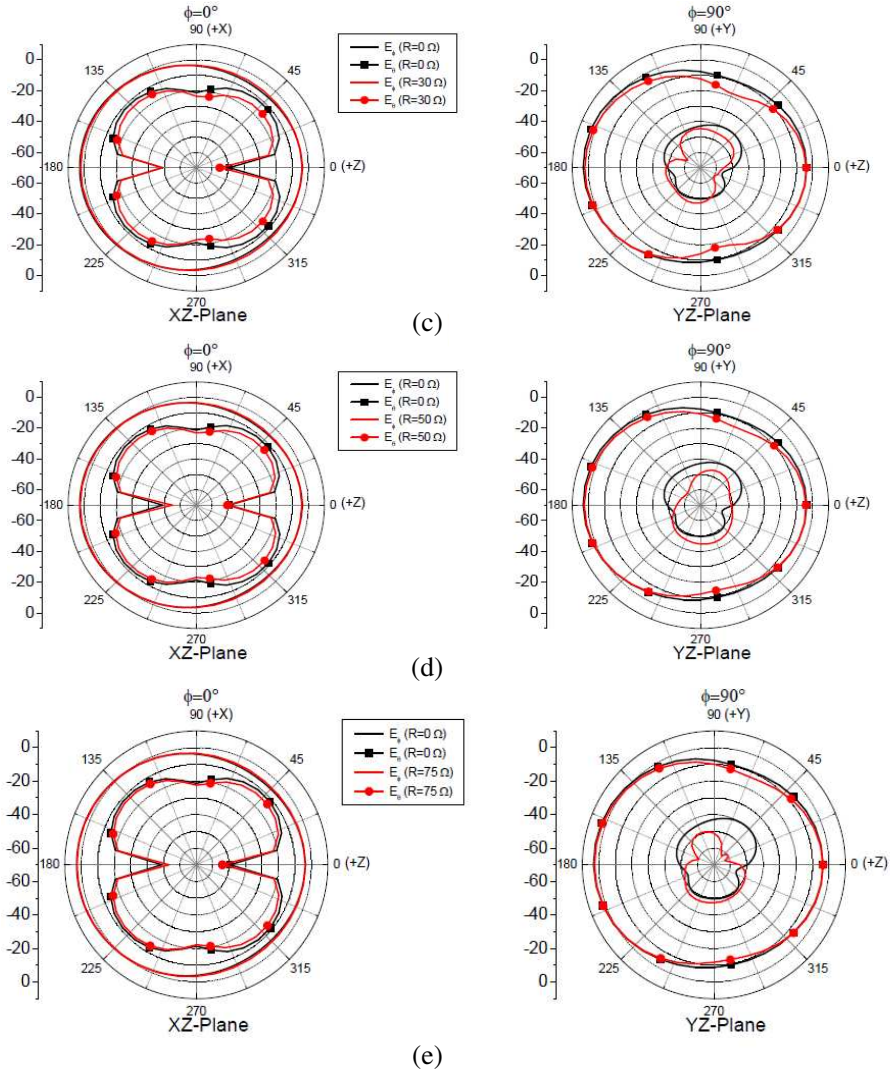

Figure 11. The measured field patterns on XZ-plane and YZ-plane of the slot patch antenna at 2.6 GHz with microstrip tuner matching impedance at (a) 0 Ω, (b) 25 Ω, (c) 30 Ω, (d) 50 Ω, (e) 75 Ω to the tuner's input impedance.

direction is the same with the E direction and the cross-polarization one is perpendicular to the E direction. In Figure 11, it is observed that the E_Φ pattern (cross-polarization) being reduced with the matching

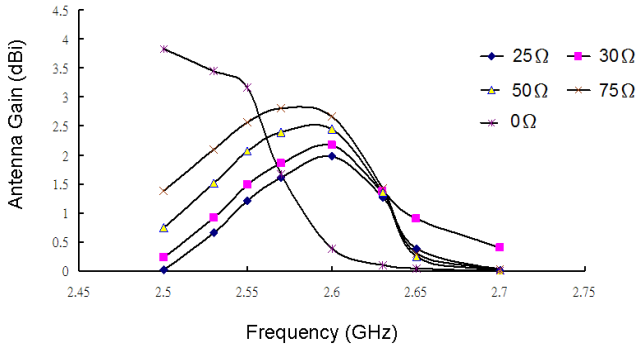

Figure 12. The measured antenna gains with dissimilar matching impedance of the tuner.

impedance. Additionally, the small value of the difference between $E_\theta \cos\Phi$ and $E_\Phi \sin\Phi$ agrees with the observations of having small radiated pattern cross-polarization (E_Φ) [35].

The circuit load of the tuner influences the bandwidth and the antenna gain significantly. In Figure 12, the antenna gains can be observed to be affected by the functional tuner at different matching impedance loads. In this study, it is realized that if the impedance is lower, the BW of the antenna will be broader; however, the antenna gain will be reduced.

4. CONCLUSION

The bandwidth and antenna gain of a slot patch antenna can be modified by adding a circuit load. If the tuner functions at the best matching impedance, it can use the power provided from the antenna through cable line to resonate at the frequency being operated. The measurements confirmed that the studied antenna with the tuner has good performance.

REFERENCES

1. Türker, N., F. Güneş, and T. Yildirim, "Artificial neural design of microstrip antennas," *Turk. J. Elec. Eng. & Comp. Sci.*, Vol. 14, No. 3, 2006.
2. Luo, Z., X. Chen, and K. Huang, "A novel electrically-small microstrip genetic antenna," *Journal of Electromagnetic Waves and Applications*, Vol. 24, No. 4, 513–520, Jan. 2010.

3. Khodae, G. F., J. Nourinia, and C. Ghobadi, "A practical miniaturized U-slot patch antenna with enhanced bandwidth," *Progress In Electromagnetics Research B*, Vol. 3, 47–62, 2008.
4. Wang, S., H. W. Lai, K. K. So, K. B. Ng, Q. Xue, and G. Liao, "Wideband shorted patch antenna with a modified half U-slot," *IEEE Antennas and Wireless Propagation Letters*, Vol. 11, 689–692, 2012.
5. Abdelaziz, A. A., "Bandwidth enhancement of microstrip antenna," *Progress In Electromagnetics Research*, Vol. 63, 311–317, 2006.
6. Zhu, F., S.-C. S. Gao, A. T. S. Ho, T. W. C. Brown, J. Li, and J.-D. Xu, "Low-profile directional ultra-wideband antenna for see-through-wall imaging applications," *Progress In Electromagnetics Research*, Vol. 121, 121–139, 2011.
7. Monavar, F. M. and N. Komjani, "Bandwidth enhancement of microstrip patch antenna using Jerusalem cross-shaped frequency selective surfaces by invasive weed optimization approach," *Progress In Electromagnetics Research*, Vol. 121, 103–120, 2011.
8. Zhang, L., Q. Zhang, and C. Hu, "The influence of dielectric constant on bandwidth of U-notch microstrip patch antenna," *IEEE International Conference on Ultra-wideband (ICUWB)*, 1–4, Nanjing, China, Sep. 2010.
9. Ahmed, O. M. H., A. R. Sebak, and T. A. Denidni, "Size reduction and bandwidth enhancement of a UWB hybrid dielectric resonator antenna for short-range wireless communications," *Progress In Electromagnetics Research Letters*, Vol. 19, 19–30, 2010.
10. Gujral, M., J. L.-W. Li, T. Yuan, and C.-W. Qiu, "Bandwidth improvement of microstrip antenna array using dummy EBG pattern on feedline," *Progress In Electromagnetics Research*, Vol. 127, 79–92, 2012.
11. Mitra, D., D. Das, and S. R. Bhadra Chaudhuri, "Bandwidth enhancement of microstrip line and CPW-FED asymmetrical slot antennas," *Progress In Electromagnetics Research Letters*, Vol. 32, 69–79, 2012.
12. Xie, J.-J., Y.-Z. Yin, J. Ren, and T. Wang, "A wideband dual-polarized patch antenna with electric probe and magnetic loop feeds," *Progress In Electromagnetics Research*, Vol. 132, 499–515, 2012.
13. Liu, X., "Bandwidth-expanded U-slot patch antenna with shorting wall," *International Symposium on Signals Systems and Electronics (ISSSE)*, 1–3, Nanjing, China, Sep. 2010.

14. Albooyeh, M., N. Kamjani, and M. Shobeyri, "A novel cross-slot geometry to improve impedance bandwidth of microstrip antennas," *Progress In Electromagnetics Research Letters*, Vol. 4, 63–72, 2008.
15. Bao, J.-H., F.-C. Ren, Q.-L. Huang, and X.-W. Shi, "A CPW-fed slotted antenna with loaded split ring for multiband applications," *Journal of Electromagnetic Waves and Applications*, Vol. 26, Nos. 11–12, 1580–1586, Aug. 2012.
16. Chen, L.-N., Y.-C. Jiao, Y. Zhu, and F.-S. Zhang, "Dual narrow band-notched ultra-wideband planar rectangular printed antenna," *Journal of Electromagnetic Waves and Applications*, Vol. 26, Nos. 2–3, 319–328, Jan. 2012.
17. Azim, R., M. T. Islam, J. S. Mandeep, and A. T. Mobashsher, "A planar circular ring ultra-wideband antenna with dual band-notched characteristics," *Journal of Electromagnetic Waves and Applications*, Vol. 26, Nos. 14–15, 2022–2032, Oct. 2012.
18. Zhou, D., S.-C. S. Gao, F. Zhu, R. A. Abd-Alhameed, and J.-D. Xu, "A simple and compact planar ultra wideband antenna with single or dual band-notched characteristics," *Progress In Electromagnetics Research*, Vol. 123, 47–65, 2012.
19. Ssorin, V., A. Artemenko, A. Sevastyanov, and R. Maslennikov, "Compact bandwidth-optimized two element MIMO antenna system for 2.5–2.7 GHz band," *Proceedings of the 5th European Conference on Antennas and Propagation*, 319–323, Rome, Italy, Apr. 2011.
20. Dahlan, A. M. M. and M. R. Kamarudin, "Shorted microstrip patch antenna with parasitic element," *Journal of Electromagnetic Waves and Applications*, Vol. 24, Nos. 2–3, 327–339, Jan. 2010.
21. Jiang, X., S. Li, and G. Su, "Broadband planar antenna with parasitic radiator," *Electronics Letters*, Vol. 39, No. 23, 2003.
22. Deng, Z.-B., W. Jiang, S.-X. Gong, Y.-X. Xu, and Y. Zhang, "A new method for broadening bandwidths of circular polarized microstrip antennas by using DGS & parasitic split-ring resonators," *Progress In Electromagnetics Research*, Vol. 136, 739–751, 2013.
23. Zhu, F., S.-C. S. Gao, A. T. S. Ho, C. H. See, R. A. Abd-Alhameed, J. Li, and J.-D. Xu, "Design and analysis of planar ultra-wideband antenna with dual band-notched function," *Progress In Electromagnetics Research*, Vol. 127, 523–536, 2012.
24. Feng, K., F. Meng, and R. Liu, "Coupled-fed monopole antenna with a parasitic open slot," *Proceedings of 2011 Cross Strait Quad-regional Radio Science and Wireless Technology*

Conference (CSQRWC 2011), 523–526, Harbin, Heilongjiang, China, Jul. 2011.

25. Yang, G., Q.-X. Chu, and Z.-H. Tu, "A compact band-notched UWB antenna with controllable notched bandwidths by using coupled slots," *Journal of Electromagnetic Waves and Applications*, Vol. 25, Nos. 14–15, 2148–2157, Jan. 2011.
26. Li, C.-M. and L.-H. Ye, "Improved dual band-notched UWB slot antenna with controllable notched bandwidths," *Progress In Electromagnetics Research*, Vol. 115, 477–493, 2011.
27. Shu, P. and Q. Feng, "Design of a compact quad-band hybrid antenna for compass/WiMAX/WLAN applications," *Progress In Electromagnetics Research*, Vol. 138, 585–598, 2013.
28. Azini, A. S., M. R. Kamarudin, T. A. Rahman, H. U. Iddi, A. Y. Abdulrahman, and M. F. B. Jamlos, "Transparent antenna design for WiMAX application," *Progress In Electromagnetics Research*, Vol. 138, 133–141, 2013.
29. http://www.mitron.cn/product/Cables/Harbour/pdf/M17.pdf, (Data sheet of the MIL-C-17 Coaxial Cable, Harbour).
30. Lee, Y.-M., S. T. Wang, H.-C. Teng, and S. Cherng, "A functional microstrip circuit module for annular slot antenna," *Progress In Electromagnetics Research*, Vol. 136, 255–267, 2013.
31. Wang, C.-J. and Y. Dai, "Studies of power-combining of open slot antenna arrays," *Progress In Electromagnetics Research*, Vol. 120, 423–437, 2011.
32. Wu, Z. H., F. Wei, X.-W. Shi, and W.-T. Li, "A compact quad band-notched UWB monopole antenna loaded one lateral L-shaped slot," *Progress In Electromagnetics Research*, Vol. 139, 303–315, 2013.
33. Fei, P., Y. Qi, and Y.-C. Jiao, "Wide slot loop antenna with distance-adjustable back-reflector for multiple narrowband antennas replacement," *Progress In Electromagnetics Research*, Vol. 135, 563–581, 2013.
34. Trinh-Van, S., H. B. Kim, G. Kwon, and K. C. Hwang, "Circularly polarized spidron fractal slot antenna arrays for broadband satellite communications in Ku-band," *Progress In Electromagnetics Research*, Vol. 137, 203–218, 2013.
35. Koffman, I., "Feed polarization for parallel currents in reflectors generated by conic sections," *IEEE Trans. Antennas Propagation*, Vol. 14, 37–40, Jan. 1966.